

# Internal state thermometry of cold trapped molecular anions

Rico Otto,<sup>a,b,‡</sup>, Alexander von Zastrow<sup>b,‡</sup>, Thorsten Best,<sup>a</sup> and Roland Wester<sup>a,\*</sup>

Received Xth XXXXXXXXXX 20XX, Accepted Xth XXXXXXXXXX 20XX

First published on the web Xth XXXXXXXXXX 200X

DOI: 10.1039/b000000x

Photodetachment spectroscopy of  $\text{OH}^-$  and  $\text{H}_3\text{O}_2^-$  anions has been performed in a cryogenic 22-pole radiofrequency multipole trap. Measurements of the detachment cross section as a function of laser frequency near threshold have been analysed. Using this bound-free spectroscopy approach we could demonstrate rotational and vibrational cooling of the trapped anions by the buffer gas in the multipole trap. Below 50 K the  $\text{OH}^-$  rotational temperature shows deviations from the buffer gas temperature, and possible causes for this are discussed. For  $\text{H}_3\text{O}_2^-$  vibrational cooling of the lowest vibrational quantum states into the vibrational ground state is observed. Its photodetachment cross section near threshold is modelled with a Franck-Condon model, with a detachment threshold that is lower, but still in agreement with the expected threshold for this system.

## 1 Introduction

Buffer-gas cooling of trapped molecular ions has been established as a standard technique for producing cold molecules in recent years<sup>1,2</sup>. The method is efficient both for translational and for internal degrees of freedom, but precise temperature measurements have only been performed for a limited number of molecular ions. Most temperature measurements rely on high resolution spectroscopy that resolves the Doppler profile to determine the kinetic temperature of the trapped ions<sup>3–8</sup>. Effective temperatures for the internal degrees of freedom have also been determined using rotationally-resolved bound-bound spectroscopy for rotational temperatures<sup>3,9,10</sup> or, more rarely, using a vibrational hot-band analysis for the vibrational temperature<sup>11</sup>. All of these techniques rely on bound-bound action spectroscopy and are thus not applicable when efficient probing schemes are not available, which is often the case for molecular anions.

For negative molecular ions, however, photodetachment of the excess electron provides a means of action spectroscopy that is applicable to essentially all negative ions. Although at first thought it may seem surprising that the non-resonant photodetachment process, by which an electron may be lifted into the continuum as soon as the photon energy exceeds the electron affinity of the resulting neutral molecule, actually provides internal-state information on the initial anionic molecule. However, one should keep in mind that while the

detached electron may have any amount of kinetic energy, the molecular internal structure typically prevails, so that well-defined propensity rules exist for the discrete set of possible associated state-to-state transitions. The total cross-section for photodetachment at any given photon energy is thus made up of the sum of all open channels at that energy, weighted by the associated transition strengths and initial state populations. Therefore, by measuring the energy-differential cross section over a region where different channels open, we can determine the population of the corresponding initial states of the molecular anion.

In this paper we demonstrate near-threshold bound-free photodetachment spectroscopy as a thermometry scheme for molecular anions that are trapped in a multipole radio-frequency ion trap. We present results for the hydroxyl anion  $\text{OH}^-$ , one of the simplest molecular anions, and for the hydroxyl-water cluster anion  $\text{H}_3\text{O}_2^-$ , a prototype for anion-molecule clusters. The ions are subjected to buffer-gas cooling in cold helium gas, the temperature of which has been varied between ten Kelvin and room temperature.

## 2 Experimental Methods

The setup employed in these experiments has been described in parts previously<sup>22</sup>. In brief, molecular anions are produced in an electrical discharge in a pulsed gas jet, and extracted using a Wiley-McLaren type mass spectrometer. The time-of-flight selected ions are then stored in a 22-pole radio-frequency ion trap<sup>2</sup>. The trap is mounted on a closed-cycle refrigerator and is equipped with ohmic heaters and a thermal radiation shielding. This allows to fix the trap temperature anywhere between 8 K and room temperature, measured with a silicon diode thermometer. **Trapped ions are ther-**

<sup>a</sup> Institut für Ionenphysik und Angewandte Physik, Universität Innsbruck, Technikerstraße 25, A-6020 Innsbruck, Austria.

<sup>b</sup> Physikalisches Institut, Albert-Ludwigs-Universität Freiburg, Hermann-Herder-Str. 3, 79104 Freiburg, Germany.

<sup>‡</sup> Both authors contributed equally to this work. Present addresses: R. O. is now at the Department of Chemistry and Biochemistry, University of California San Diego, USA, and A. v. Z. is now at the Institute for Molecules and Materials, Radboud University Nijmegen, The Netherlands

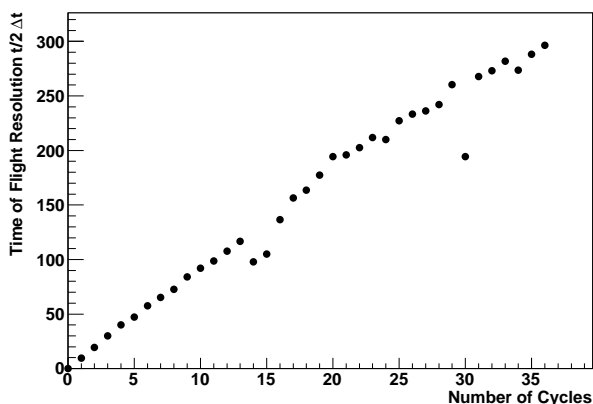


**Fig. 1** Measured time resolution of  $\text{OH}^-$  ions after a selected number of round trips in the multicycle reflectron mass spectrometer. Plotted is half of the time-of-flight resolution, which directly represents the mass resolution achieved with the device.

malized by collisions with an inert buffer gas (helium) that is applied into the trap enclosure at typical densities of  $10^{14} \text{ cm}^{-3}$  leading to  $10^4 - 10^5$  collisions per second.

After an initial thermalisation time of 10 ms, the anions are exposed to a laser beam propagating along the trap axis for the selected exposure time, after which the remaining ions are detected using the same time-of-flight mass spectrometer. By varying the exposure time, we measure the laser-induced ion loss rate, which is directly proportional to the energy-differential photodetachment cross section at the given photon energy. The full energy-differential cross section is determined by tuning the laser wavelength, which is referenced to a high-resolution wavemeter. The laser light is derived from external cavity red diode lasers for photodetachment of  $\text{OH}^-$  anions, and free-running blue-ray diode lasers for  $\text{H}_3\text{O}_2^-$ , which have been built in-house. In either case, the lasers can be tuned over several nanometres using temperature tuning. By coupling the laser light through a single-mode optical fibre temperature-induced drifts of the beam pointing are suppressed. Therefore, the laser always illuminates the same spot within the ion cloud, and a full tomographic measurement<sup>14,15,22</sup> at every laser wavelength is not required for the relative cross section measurements.

The ions that remain in the trap after being exposed to the photodetachment laser, are extracted from the trap and detected. In order to distinguish different ionic species the ions enter a multicycle reflectron time-of-flight mass spectrometer. This device consists of two coaxial reflectron mirrors that are placed 460 mm apart, similar to a resonator ion trap<sup>23,24</sup>. While the rear mirror is held on a repulsive potential the front mirror is grounded as the ion packet enters the device. As this mirror is switched to a repulsive potential as well, the ion

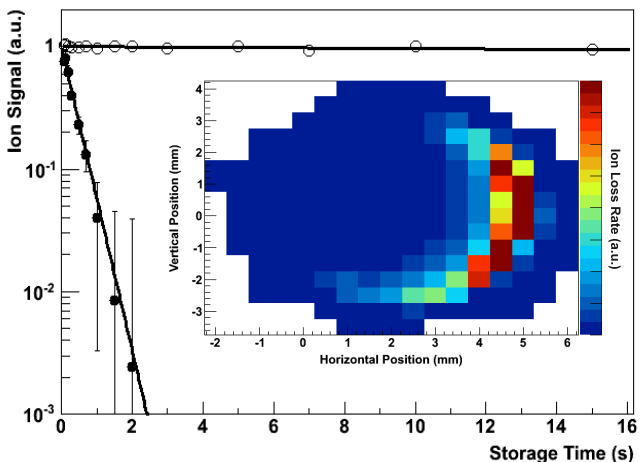


**Fig. 2** Laser-induced trap loss of  $\text{OH}^-$  above the  $J = 0$  photodetachment threshold. All rotational states contribute to this decay channel. The inset shows a two-dimensional tomography scan, which represents the column density of the ions in the 22-pole trap (see methods).

packet becomes confined in the multicycle reflectron and travels back and forth between the two mirrors at a fixed mass dependent frequency. Since in a time-of-flight arrangement the mass resolution  $m/\Delta m = t/2\Delta t$  is directly depending on the flight time, the multicycle reflectron design offers an elegant way to achieve a desired mass resolution by confining the ions for a given number of cycles. Fig. 1 displays the mass resolution for  $\text{OH}^-$  achieved using the multicycle reflectron as a function of the first 35 cycles. When the desired mass resolution is achieved the ion packet is released by switching the front mirror to ground again. The ions leave the device and get detected on a multi channel plate ion detector.

### 3 Results and Discussion

#### 3.1 Near-threshold photodetachment of $\text{OH}^-$

For the hydroxyl molecular anion  $\text{OH}^-$  in the radiofrequency 22-pole ion trap, the vibrational motion can be considered to be frozen out completely (i. e. there is on average far less than one excited-state ion present in the trap) already at room temperature. At low temperatures we therefore only have to deal with rotational excitations of an approximately rigid rotor with a rotational constant of  $B_0 = 18.735 \text{ cm}^{-1}$ <sup>12</sup>. At 50 K, rotational levels up to  $J = 2$  are populated to a measurable degree. Measurements have therefore been performed for a range of photon energies covering the thresholds of the lowest three rotational states, as described in the experimental methods section below.

The threshold for photodetachment of ground state ( $J = 0$ )

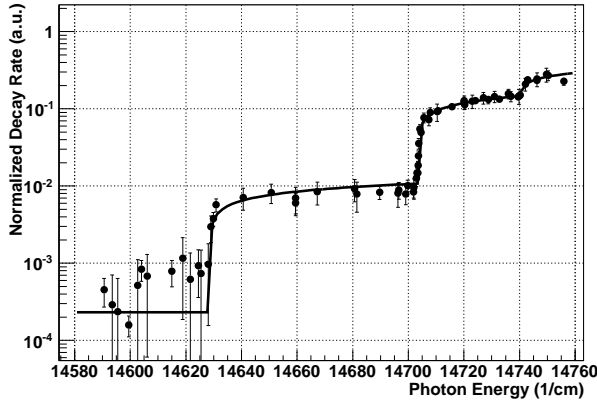


**Fig. 3** Photodetachment cross section of  $\text{OH}^-$  at a trap temperature of 50 K for varying photon energy. The steps in the cross section are due to the opening of loss channels corresponding to the  $J = 2, 1$  and 0 rotational states of the anion.

hydroxyl anions lies at  $14740.982(7)\text{cm}^{-1}$ , the electron affinity of neutral  $^{16}\text{O}^1\text{H}^{13}$ . When tuning the photodetachment laser to a slightly larger photon energy, photodetachment dominates the ion loss from the trap, as shown in Fig. 2. The long background lifetime of the ions in the trap of more than  $10^3$  s allows for photodetachment rate measurements over several orders of magnitude. The inset in Fig. 2 shows a two-dimensional tomography scan of the spatial density of the trapped ion cloud, which is used in the determination of absolute photodetachment cross sections<sup>14,15</sup>.

For photon energies below the  $J = 0$  detachment threshold, only rotationally excited hydroxyl anions can be detached. The measured relative rate of photodetachment of the trapped ions is plotted in Fig. 3 as a function of the photon energy, which is tuned across the detachment thresholds for the first three rotational states. The scan was obtained for a helium buffer gas temperature of 50 K. The thresholds for the states with  $J = 0, 1$ , and 2 are clearly observed. They are assigned to the openings of the photodetachment transitions  $\text{R3}(0)$ ,  $\text{Q3}(1)$ , and  $\text{P3}(2)$  (for the notation see Ref.<sup>13</sup>) transitions, which all form neutral OH in the rotational ground state of the  $^2\Pi_{3/2}$  spin-orbit manifold. Thus, the energy difference between the thresholds represents directly the rotational levels in the molecular anion, which are known from rotational spectroscopy<sup>12</sup> to be given by  $37.5\text{cm}^{-1}$  for the  $J = 1 \leftarrow 0$  excitation and  $112.3\text{cm}^{-1}$  for the  $J = 2 \leftarrow 0$  excitation, respectively. The measured differences of the thresholds agree very well with this prediction.

The shape of the cross section near threshold, more specifically the relative heights of the components that terminate at the different thresholds, is determined by the population of the different rotational states of the anion. To describe the shape

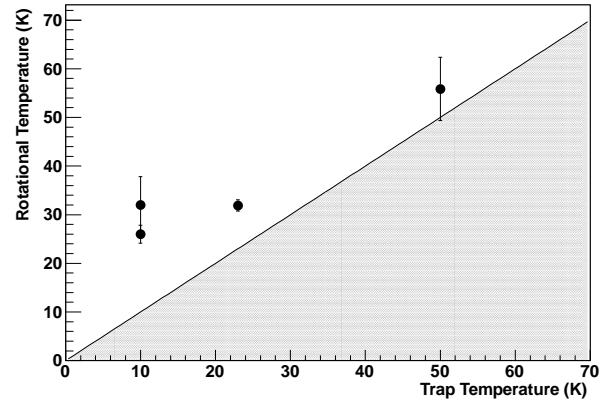


**Fig. 4** Rotational temperatures of  $\text{OH}^-$  anions determined from the ratio of the observed photodetachment transitions originating in  $J = 1$  and  $J = 2$  levels, respectively, for different temperatures of the helium buffer gas in the 22-pole trap.

of the cross section we employ the functional form

$$\sigma(h\nu) \propto \sum_J P(J) I_J (h\nu - \varepsilon_J)^p, \quad (1)$$

where  $h\nu$  is the photon energy,  $P(J)$  is the population of the rotational levels of the hydroxyl anion,  $I_J$  and  $\varepsilon_J$  are the corresponding Hönl-London factors (taken from Ref.<sup>13</sup>) and threshold energies, and  $p$  is the exponent for the power law describing the energy dependence of the cross section near threshold. For a non-interacting outgoing s-wave electron  $p = 0.5$ , corresponding to the Wigner threshold law. In the present case the electron-dipole coupling modifies the power law<sup>16</sup>. For this scenario the exponent has been derived to be  $p = 0.28$ <sup>17</sup>.

By fitting Eq. 1 to the measured cross section in Fig. 3, we obtain the population in the rotational levels  $J = 0 \dots 2$ . When leaving  $p$  as free parameters in the fit, we obtain  $p_P = 0.23(4)$  and  $p_Q = 0.30(2)$  for the P- and Q-branches, respectively. As these values are in good agreement with the value derived in Ref.<sup>17</sup>, we fix the parameter to the latter value  $p = 0.28$  to improve the stability of the fit. This leaves the rotational populations as the only free fit parameters. From the population ratio of two rotational states the rotational temperature can be derived. The most precise evaluation is based on the ratio of molecules in  $J = 2$  and  $J = 1$ , since these two thresholds have been covered best in the frequency scan. This yields a rotational temperature of  $57 \pm 6$  K for the data in Fig. 3, in reasonable agreement with the helium buffer gas temperature of 50 K.

Further spectroscopic scans of the photodetachment rate near threshold have been performed for buffer gas temperatures of 10 and 23 K and the spectra have also been fit with Eq.

1. Fig. 4 compares the obtained rotational temperatures to the buffer gas temperatures in the corresponding measurements. While at higher temperatures, the temperatures agree roughly within the experimental uncertainty, a significant deviation is found for lower temperatures, where the ion temperature always exceeds the buffer gas temperature.

Different causes may be responsible for this deviation. Radiofrequency heating due to collisions with buffer gas atoms in the presence of the radiofrequency field is known to increase the translational temperature of trapped ions. This will indirectly also affect the rotational temperature. However, this effect is suppressed in traps with a high multipole order such as the employed 22-pole trap to the level of a few percent<sup>1,2</sup>. It may, however, play a larger role if the effective potential is disturbed by surface patch potentials or by pockets that are induced by slight geometrical distortions of the trap electrodes<sup>18</sup>. The two different rotational temperatures measured for 10 K buffer gas temperature in Fig. 4, even though barely statistically significant, may be caused by different patch potential conditions in the ion trap. A second possible mechanism is the direct rotational excitation by room temperature blackbody radiation that enters the trap via its entrance and exit electrodes. Incomplete thermalisation can be excluded, because many hundred to a few thousand buffer gas collisions have occurred even for the shortest storage times that we employed in the measurements. In the future, we will carry out further investigations by varying the trapping potentials and the buffer gas conditions in the trap, in order to clarify the source of the observed rotational heating.

### 3.2 Near threshold photodetachment of $\text{H}_3\text{O}_2^-$

**For small molecular systems where the rotational structure can be clearly resolved the above method should be of general use. In order to test the applicability for larger molecules and probe its sensitivity on vibrational cooling the photodetachment thermometry method is now applied to a more complex molecular system.**

$\text{H}_3\text{O}_2^-$  is a model system for a molecular cluster that may rotate and vibrate even at low temperatures, because of several low-frequency vibrational modes. It represents the smallest deprotonated water cluster, small enough that full nine-dimensional Born-Oppenheimer potential calculation and detailed quantum calculations of the fundamental vibrational frequencies have been carried out<sup>19,20</sup>. It has been found that the ground state structure of  $\text{H}_3\text{O}_2^-$  is an inversion-symmetric bent configuration with the central proton shared between hydroxyl anions. As a consequence, the low-frequency vibrational modes are split due to tunnelling.

The threshold for ground state  $\text{H}_3\text{O}_2^-$  photodetachment lies near 3.0 eV or about  $24200\text{ cm}^{-1}$ , based on the electron affinity of OH of 1.82 eV and the dissociation energy of  $\text{H}_3\text{O}_2^-$  of

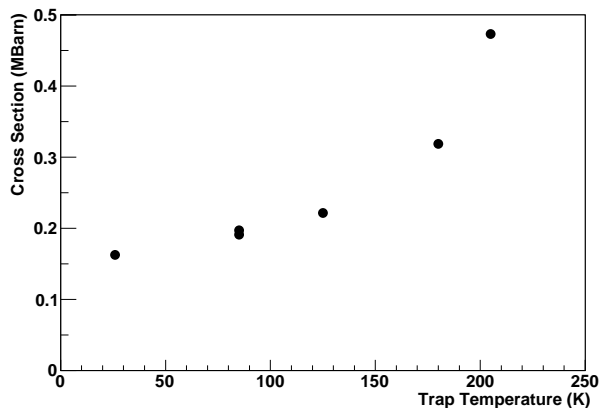


**Fig. 5** Photodetachment cross section of  $\text{H}_3\text{O}_2^-$  at a photon energy of  $24410 \pm 20\text{ cm}^{-1}$  for different trap temperatures (1 MBarn =  $10^{-18}\text{ cm}^2$ ). An independent full 2D tomographic measurement has been performed at each temperature.

$1.18\text{ eV}^{21}$  and neglecting possible bound states in the neutral OH-water complex. We have therefore measured the near-threshold photodetachment cross sections at a fixed photon energy of  $24410 \pm 20\text{ cm}^{-1}$  for trap temperatures of 30, 85, 130, 180 and 205 K respectively, using the tomographic procedure outlined in the methods section. The result is shown in Fig. 5. At room temperature, where we could only complete a partial tomography due to the increase in width of the density distribution, we estimate a cross section of  $1.5 \pm 0.5\text{ MBarn}$  (1 MBarn =  $10^{-18}\text{ cm}^2$ ) by extrapolation. The data in Fig. 5 show a strong increase of the cross section with temperature, which also requires a strong dependence of the detachment cross section on the internal quantum state. In turn, the change in cross section also shows that cooling of these internal quantum states actually takes place when lowering the buffer gas temperature from room temperature down to 30 K.

To gain further insight, the photodetachment cross section is measured as a function of the laser frequency in the vicinity of the detachment threshold. The results are plotted in Fig. 6 for temperatures of 30, 85, 130, 205 and 300 K, respectively. For all temperatures the cross section increases with a nearly linear photon energy dependence and with an apparent threshold of about  $24000\text{ cm}^{-1}$ . The tuning range of the employed diode laser was limited to energies above  $24150\text{ cm}^{-1}$ , which prevented measurements closer to this apparent threshold. Nevertheless it becomes evident that the energy dependence of the cross section is quite different from that for bare  $\text{OH}^-$ . Describing it with a function proportional to  $(h\nu - E_0)^p$  near an energy threshold  $E_0$ , the data suggests  $p$  to be approximately 1 for  $\text{H}_3\text{O}_2^-$  and not about 0.28 as found for  $\text{OH}^-$  or 0.5 for pure s-wave detachment. This can not be easily explained by the electronic structure of the  $\text{H}_3\text{O}_2^-$  complex, and is more likely

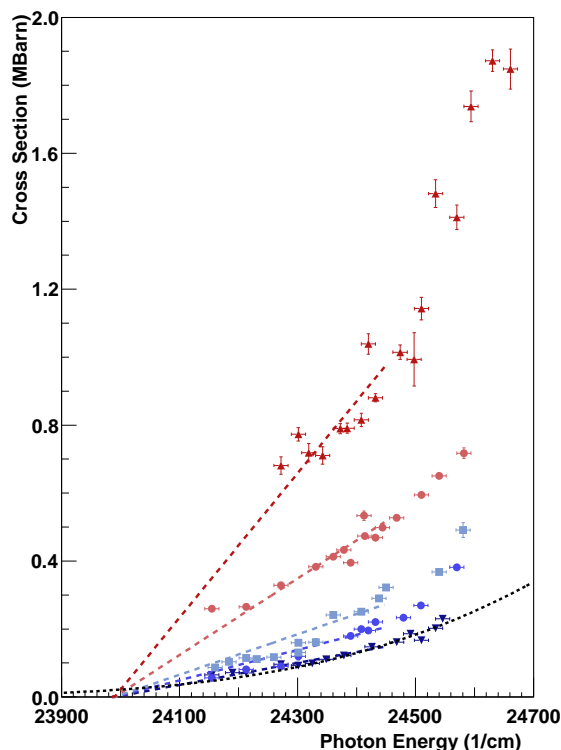


**Fig. 6** Near threshold photodetachment scans of  $\text{H}_3\text{O}_2^-$  for temperatures of 30, 85, 130, 205 and 300 K, respectively (from bottom to top and from dark blue to dark red). Each measurement is based on a partial tomography of the cloud density, scaled according to a single full tomography at each temperature. The straight dashed lines represent simple linear extrapolations of the cross sections to identify the apparent photodetachment threshold. The black dotted line is the result of our Franck-Condon model for the detachment of ground state  $\text{H}_3\text{O}_2^-$  and agrees well with the data for 30 K.

caused by its internal structure, as discussed below.

For all studied temperatures in Fig. 6 a linear extrapolation fits the data well. The intercept of this extrapolation with the photon energy axis is approximately the same for all temperatures and its value of about  $24000\text{ cm}^{-1}$  agrees well with the expected threshold of  $24200\text{ cm}^{-1}$ , in particular when considering that the latter value has an estimated accuracy of several hundred wavenumbers. The slope, however, changes significantly, which is again a signature of cooling of the internal temperature of the trapped  $\text{H}_3\text{O}_2^-$  anions at the different buffer gas temperatures. Specifically, it can be caused by the changes of the rotational or vibrational state population. The rotational states are very closely spaced, given the rotational constants of  $\text{H}_3\text{O}_2^-$  of 10, 0.3 and  $0.3\text{ cm}^{-1}$ <sup>20</sup>. Therefore all dipole-allowed detachment transitions are also energetically allowed at the photon energies of the measurement. The Hönl-London

factors for all dipole-allowed photodetachment transitions of a specific rotational state of the anion are assumed to sum up to unity, similar to the case for  $\text{OH}^-$  where this renders the absolute photodetachment cross section independent of temperature<sup>15</sup>. This implies that a change of the rotational population due to lowering the temperature will not have an influence on the measured cross section. The observed change therefore has to be attributed to vibrational cooling of the cluster anion and not to rotational cooling.

The lowest vibrational frequencies of the cluster are two frequencies  $\omega_+$ ,  $\omega_-$  of the torsional mode of about 132 and  $215\text{ cm}^{-1}$ , which are split due to tunnelling between different equivalent structures on the Born-Oppenheimer potential surface<sup>20</sup>. At 30 K one expects from Boltzmann statistics about 0.1% in the lowest excited vibrational state. Even if the vibrational temperature of the anions were several Kelvin larger than the buffer gas temperature, which may occur due to trap imperfections and radiofrequency heating (see also the discussion in section 3.1)<sup>2</sup>, still no substantial population in any of the excited state is expected. Then at 85 K about 11% of the anions should be found with one of the two torsional modes excited. Higher-frequency vibrational modes and also overtones of the low frequencies only become populated at higher temperatures. At 200 K many states are populated, but due to the lack of knowledge on the eigenenergies of the overtone states we did not calculate populations for this temperature.

For the two torsional eigenstates, which are symmetric and antisymmetric linear combinations of two localised torsional modes, we assume that their Franck-Condon factors upon photodissociation to the neutral  $\text{OH-H}_2\text{O}$  system, which subsequently dissociates into  $\text{OH}$  and  $\text{H}_2\text{O}$ , are the same. One can then use the measured detachment cross sections for 30 K and 85 K, which increase by about a factor of 1.2 (see Fig. 5), to extract that the 11% torsionally excited anions should have about a threefold enhanced detachment cross section compared to vibrational ground state clusters.

To understand the threshold behaviour of the cross section we have developed a qualitative Franck Condon model. A full theoretical model, which would be required in order to use the presented measurements for calibration-independent vibrational thermometry, is beyond the scope of this work. Here we restrict ourselves to a one-dimensional description along the O-O direction and assume that upon photodetachment the neutral molecule will dissociate primarily along this direction. We fix all other coordinates to the equilibrium values for the anion **that were obtained from a MP2/aug-cc-PVDz geometry optimization** and assume that no significant geometry changes along orthogonal directions occur upon photodetachment. **Our calculation does not account for zero point energy which is a prerequisite to find the symmetric  $(\text{HO}\cdots\text{H}\cdots\text{OH})^-$  anion geometry. Instead the equilibrium structure used in this model is described**

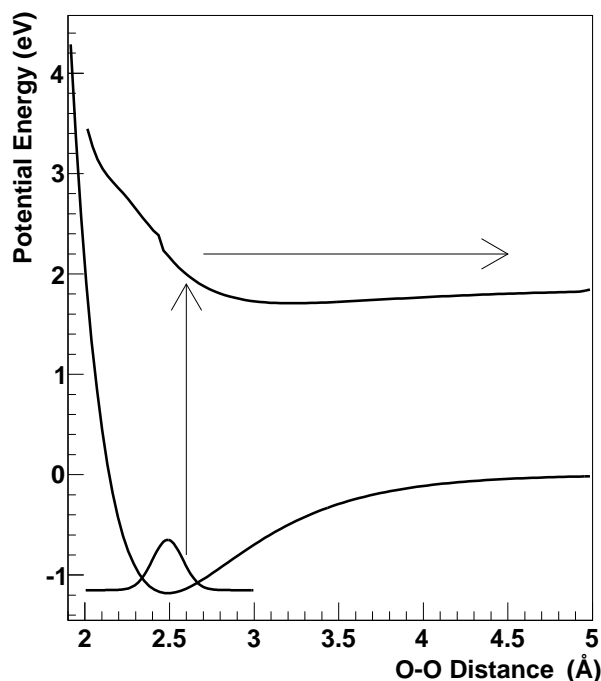


**Fig. 7** Franck-Condon model for the photodetachment threshold behaviour based on the variation of potential energy along the O-O stretch coordinate. The Franck Condon overlap is determined by the ground state wavefunction at the Condon point corresponding to the incoming photon and released electron energy. The energy threshold for photodetachment into the dissociative continuum is determined from the  $\text{H}_3\text{O}_2^-$  dissociation energy  $E_{\text{diss}}$  and the hydroxyl electron affinity  $EA$ . The neutral potential curve was taken from an ab initio calculation.

**by a  $\text{OH}^-(\text{H}_2\text{O})$  cluster geometry.** A sketch of the relevant potential curves in this one-dimensional model is shown in Fig. 7. The anion ground state wavefunction is centred around the equilibrium distance at 2.4896 Å. It can be approximated by a Gaussian with an r.m.s. width calculated from the eigenfrequency of the O-O stretch mode of  $515\text{ cm}^{-1}$ <sup>20</sup>. The energy difference between the anion ground state and the neutral asymptote  $\text{OH} + \text{H}_2\text{O}$  is assumed to be 3.0 eV or  $24200\text{ cm}^{-1}$ <sup>21</sup>. To obtain the potential curve for the dissociating neutral complex, we have performed one-dimensional ab initio potential energy calculations at the CCSD(T) level of theory in the aug-cc-PVDz basis. Neglecting zero-point energies, this potential is also shown in Fig. 7, it features a shallow minimum around  $\approx 3.2\text{ Å}$ . In the range between 2.1 Å and 2.7 Å, the ab initio potential is repulsive and lies higher in energy than the asymptote.

The photodetachment cross section depends on the Franck-

Condon overlap between the anion and neutral vibrational wavefunctions and on the amount of excess energy that is released to the free electron. As the Franck-Condon overlap with the bound neutral states residing in the shallow potential well is small, detachment into bound states is expected to be negligible. The neutral wavefunctions in the dissociation continuum are simplified by delta functions at the inner turning points of the potential. The Franck-Condon factor then becomes the square of the anion vibrational wavefunction at a fixed O-O distance. The excess energy taken by the electron is given by the difference between the photon energy, the threshold energy for photodetachment and the repulsive energy between the neutral fragments. As the photon energy is increased, larger repulsive energies can be reached, so that smaller O-O distances become accessible for photodetachment. Due to the Franck Condon factor this enhances the cross section much more than it is reduced by the decreasing electron excess energy. Qualitatively, this causes the approximately linear increase of the cross sections in Fig. 6.

More specifically, the photodetachment cross section can be obtained by integrating over all contributing O-O distances. Using a similar threshold scaling for the electron kinetic energy as for OH in the previous section (see Eq. 1), the cross section here is given by

$$\sigma(h\nu) \propto \int_{(h\nu - E_0 - V(r)) > 0} |\psi(r)|^2 (h\nu - E_0 - V(r))^p dr, \quad (2)$$

where  $h\nu$  is again the photon energy,  $E_0$  is the energy threshold of the cluster,  $V(r)$  is the repulsive potential of the neutral complex, and  $\psi(r)$  is the anion wave function as a function of the O-O distance  $r$ . For the exponent  $p$  we assume 0.5 for s-wave electron detachment, which should be a better assumption here than for  $\text{OH}^-$  due to the vanishing electric dipole moment of the inversion symmetric ground state of  $\text{H}_3\text{O}_2^-$ . The result of this model is overlaid with the 30 K data in Fig. 6, where both a reduction of the energy threshold to  $23700\text{ cm}^{-1}$  and a scaling factor had to be applied to fit to the experimental data. Qualitatively, the model reproduces the shape of the 30 K data, identified as photodetachment from the vibrational ground state of the anion. Also the asymptotic cross section for photon energies high above threshold where the Franck-Condon factor approaches unity falls into the same order of magnitude of  $10^{-17}\text{ cm}^2$  as for  $\text{OH}^-$ . The lowering of the energy threshold by  $500\text{ cm}^{-1}$  can either be caused by the finite accuracy of the neutral potential calculation or by the uncertainty of the dissociation energy of the anion. In future work it would be desirable to independently obtain either  $E_0$  or  $V(r)$  with higher accuracy, because then the detachment data can be used to put stronger constraints on either the dissociation energy of the  $\text{H}_3\text{O}_2^-$  cluster or the dissociative potential of the  $\text{OH} + \text{H}_2\text{O}$  collision system.

Upon increasing the temperature to 85 K, the tunnelling

doublet of the torsional mode becomes excited. To first approximation, this leaves the shape of the ground state wavefunction of the O-O-stretch mode unaffected. In this situation, a  $\Delta v_{\text{torsion}} = -1$  photodetachment transition becomes possible, which allows for a larger electron kinetic energy. Although the Franck-Condon overlap is supposedly small for this type of transition, the extra electron energy may increase the total cross section. The one-dimensional model described above can not treat this case. A quantitative evaluation of the change in cross section for the torsionally excited vibrational states already requires a multi-dimensional calculation beyond the scope of this work. As temperatures increase beyond 100 K, overtones of the torsional mode become excited. At this point, even qualitative predictions are difficult, as the corresponding energies and wavefunctions are largely unknown. Furthermore, it seems conceivable that also rotational excitation may affect the Franck Condon overlap and thereby the cross section by means of centrifugal stretching of the O-H-O bonds.

## 4 Conclusion

We have shown that near-threshold photodetachment spectroscopy of trapped and buffer gas cooled molecular anions is capable of measuring internal state populations. This will allow further investigations of the efficiency of thermalisation of the rotational and vibrational degrees of freedom by buffer gas cooling under different trapping conditions. The information is also useful for internal state-dependent collision and reaction studies, and has recently already been employed in reactions of  $\text{H}_3\text{O}_2^-$  with  $\text{CH}_3\text{I}$ <sup>25,26</sup>. Furthermore, photodetachment spectroscopy is an important prerequisite for high resolution terahertz spectroscopy of low-lying rotational and vibrational states in such systems, because it allows for action spectroscopic detection of internal excitations on the few-molecule level. While our method is in principle quite general and can be applied to essentially any anionic species, a sufficient understanding of the molecular structure of both the anion and the corresponding neutral is necessary.

## 5 Acknowledgements

R.O. acknowledges support by the Landesgraduiertenförderung Baden-Württemberg. This work is supported by the European Research Council under ERC grant agreement No. 279898. We thank Matthias Weidemüller for many stimulating discussions and Petr Hlavenka

and Sebastien Jézouin for their help during preliminary experiments. We also thank the University of Freiburg, where the measurements presented here have been carried out, for supporting this research.

## References

- 1 O. Asvany and S. Schlemmer, *Int. J. Mass. Spectrom.*, 2009, **279**, 147.
- 2 R. Wester, *J. Phys. B*, 2009, **42**, 154001.
- 3 S. Schlemmer, T. Kuhn, E. Lescop and D. Gerlich, *Int. J. Mass Spectrom.*, 1999, **185-187**, 589.
- 4 J. Mikosch, H. Kreckel, R. Wester, R. Plasil, J. Glosik, D. Gerlich, D. Schwalm and A. Wolf, *J. Chem. Phys.*, 2004, **121**, 11030.
- 5 J. Glosik, P. Hlavenka, R. Plasil, F. Windisch, D. Gerlich, A. Wolf and H. Kreckel, *Phil. Trans. R. Soc. A*, 2006, **364**, 2931.
- 6 O. Asvany, E. Hugo, F. Müller, F. Kühnemann, S. Schiller, J. Tennyson and S. Schlemmer, *J. Chem. Phys.*, 2007, **127**, 154317.
- 7 H. Kreckel, D. Bing, S. Reinhardt, A. Petrignani, M. Berg and A. Wolf, *J. Chem. Phys.*, 2008, **129**, 164312.
- 8 O. Asvany, O. Ricken, H. S. P. Müller, M. C. Wiedner, T. F. Giesen and S. Schlemmer, *Phys. Rev. Lett.*, 2008, **100**, 233004.
- 9 S. Schlemmer, E. Lescop, J. von Richthofen, D. Gerlich and M. A. Smith, *J. Chem. Phys.*, 2002, **117**, 2068.
- 10 A. Dzhonson, D. Gerlich, E. J. Bieske and J. P. Maier, *J. Mol. Struct.*, 2006, **795**, 93–97.
- 11 J. A. Stearns, S. Mercier, C. Seaiby, M. Guidi, O. V. Boyarkin and T. R. Rizzo, *J. Am. Chem. Soc.*, 2007, **129**, 11814.
- 12 F. Matsushima, T. Yonezu, T. Okabe, K. Tomaru and Y. Moriwaki, *J. Mol. Spectrosc.*, 2006, **235**, 261.
- 13 F. Goldfarb, C. Drag, W. Chaibi, S. Kröger, C. Blondel and C. Delsart, *J. Chem. Phys.*, 2005, **122**, 014308.
- 14 S. Trippel, J. Mikosch, R. Berhane, R. Otto, M. Weidemüller and R. Wester, *Phys. Rev. Lett.*, 2006, **97**, 193003.
- 15 P. Hlavenka, R. Otto, S. Trippel, J. Mikosch, M. Weidemüller and R. Wester, *J. Chem. Phys.*, 2009, **130**, 061105.
- 16 J. R. Smith, J. B. Kim and W. C. Lineberger, *Phys. Rev. A*, 1997, **55**, 2036.
- 17 P. Engelking, *Physical Review A*, 1982, **26**, 740–745.
- 18 R. Otto, P. Hlavenka, S. Trippel, J. Mikosch, K. Singer, M. Weidemüller and R. Wester, *J. Phys. B*, 2009, **42**, 154007.
- 19 X. Huang, B. Braams, S. Carter and J. Bowman, *J. Am. Chem. Soc.*, 2004, **126**, 5042–5043.
- 20 A. B. McCoy, X. C. Huang, S. Carter and J. M. Bowman, *J. Chem. Phys.*, 2005, **123**, 064317.
- 21 D. W. Arnold, C. Xu and D. M. Neumark, *The Journal of Chemical Physics*, 1995, **102**, 6088.
- 22 T. Best, R. Otto, S. Trippel, P. Hlavenka, A. von Zastrow, S. Eisenbach, S. Jezouin, R. Wester, E. Vigren, M. Hamberg and W. D. Geppert, *Ap. J.*, 2011, **742**, 63.
- 23 D. Zajfman, O. Heber, L. Vejby-Christensen, I. Ben-Itzhak, M. Rappaport, R. Fishman and M. Dahan, *Phys. Rev. A*, 1997, **55**, 1577.
- 24 M. Dahan, R. Fishman, O. Heber, M. Rappaport, N. Altshtein, W. van der Zande and D. Zajfman, *Rev. Sci. Instrum.*, 1998, **69**, 76.
- 25 R. Otto, J. Brox, M. Stei, S. Trippel, T. Best and R. Wester, *Nature Chemistry*, 2012, **4**, 534.
- 26 R. Otto, J. Xie, J. Brox, S. Trippel, M. Stei, T. Best, M. R. Siebert, W. L. Hase and R. Wester, *Faraday Discuss.*, 2012, Advance Article.